frontiers in Ecology and Evolution

ORIGINAL RESEARCH
published: 06 September 2021
doi: 10.3389/fevo.2021.661216

# Functional Analyses of Peripheral Auditory System Adaptations for Echolocation in Air vs. Water

*Darlene R. Ketten[1,2]*, James A. Simmons[3,4], Hiroshi Riquimaroux[5,6] and Andrea Megela Simmons[4,7]*

*[1] Department of Biology, Woods Hole Oceanographic Institution, Woods Hole, MA, United States, [2] Department of Biomedical Engineering, Hearing Research Center, Boston University, Boston, MA, United States, [3] Department of Neuroscience, Brown University, Providence, RI, United States, [4] Carney Institute for Brain Science, Brown University, Providence, RI, United States, [5] Shandong University-Virginia Tech International Laboratory, Shandong University, Jinan, China, [6] National Hospital Organization Tokyo Medical Center, Tokyo, Japan, [7] Department of Cognitive, Linguistic, and Psychological Sciences, Brown University, Providence, RI, United States*

The similarity of acoustic tasks performed by odontocete (toothed whale) and microchiropteran (insectivorous bat) biosonar suggests they may have common ultrasonic signal reception and processing mechanisms. However, there are also significant media and prey dependent differences, notably speed of sound and wavelengths in air vs. water, that may be reflected in adaptations in their auditory systems and peak spectra of out-going signals for similarly sized prey. We examined the anatomy of the peripheral auditory system of two species of FM bat (big brown bat *Eptesicus fuscus;* Japanese house bat *Pipistrellus abramus*) and two toothed whales (harbor porpoise *Phocoena phocoena;* bottlenose dolphin *Tursiops truncatus*) using ultra high resolution (11–100 micron) isotropic voxel computed tomography (helical and microCT). Significant differences were found for oval and round window location, cochlear length, basilar membrane gradients, neural distributions, cochlear spiral morphometry and curvature, and basilar membrane suspension distributions. Length correlates with body mass, not hearing ranges. High and low frequency hearing range cut-offs correlate with basilar membrane thickness/width ratios and the cochlear radius of curvature. These features are predictive of high and low frequency hearing limits in all ears examined. The ears of the harbor porpoise, the highest frequency echolocator in the study, had significantly greater stiffness, higher basal basilar membrane ratios, and bilateral bony support for 60% of the basilar membrane length. The porpoise's basilar membrane includes a "foveal" region with "stretched" frequency representation and relatively constant membrane thickness/width ratio values similar to those reported for some bat species. Both species of bats and the harbor porpoise displayed unusual stapedial input locations and low ratios of cochlear radii, specializations that may enhance higher ultrasonic frequency signal resolution and deter low frequency cochlear propagation.

**Keywords: biosonar, cochlea, basilar membrane, stapes, inner ear, echolocation, bat, dolphin**

OPEN ACCESS

***Edited by:***
*Fernando Montealegre-Z, University of Lincoln, United Kingdom*

***Reviewed by:***
*Arthur Popper, University of Maryland, College Park, United States*
*Jakob Christensen-Dalsgaard, University of Southern Denmark, Denmark*

****Correspondence:***
*Darlene R. Ketten*
*dketten@whoi.edu*

***Specialty section:***
*This article was submitted to Behavioral and Evolutionary Ecology, a section of the journal Frontiers in Ecology and Evolution*

***Received:*** *30 January 2021*
***Accepted:*** *23 July 2021*
***Published:*** *06 September 2021*

***Citation:***
*Ketten DR, Simmons JA, Riquimaroux H and Simmons AM (2021) Functional Analyses of Peripheral Auditory System Adaptations for Echolocation in Air vs. Water. Front. Ecol. Evol. 9:661216. doi: 10.3389/fevo.2021.661216*

## INTRODUCTION

The adaptive importance of detecting sound cues is underscored by the universality of "hearing." There are lightless habitats on earth with naturally blind animals, but no terrestrial habitat is without sound, and no known vertebrate is naturally profoundly deaf. Mechanistically, hearing is conceptually a relatively simple chain of events: sound energy is received and converted by biomechanical transducers (middle and/or inner ear) into electrical signals (neural impulses) that provide a central processor (brain) with acoustic data. The complexity of these structures varies considerably by taxa, from relatively simple acoustic pressure detectors to the typical mammalian ear which packs over 75,000 mechanical and electrochemical components into an average volume of 1 $cm^3$. The focus of this paper is on comparisons of ears of two mammalian groups, microchiropteran bats and odontocete cetaceans, both of which are echolocators.

Inner ear anatomy is similar across all mammals. There is a tri-chambered spiral cochlear labyrinth with a major partition, the basilar membrane, which functions as a tonotopic resonator and that supports the organ of Corti. Hair cells and supporting cells in the organ of Corti are the primary transducers of acoustic energy into neural impulses and which also control intracochlear afferent and efferent responses. Variations in the structure and number of these ear components account for most of the differences in hearing capacity among mammals (Echteler et al., 1994; Ekdale, 2016). In particular, basilar membrane dimensions, membrane support structures, cochlear spiral configurations, and neural densities and distributions have been proposed as critical determinants of hearing range and sensitivity (von Békésy, 1960; West, 1985; Greenwood, 1990; Heffner and Heffner, 1992). Further analyses of these variations also led to the designations of "generalist" and "specialist" ears (Fay, 1988; Echteler et al., 1994), the latter referring primarily to differences in the structure of the basilar membrane that affect stiffness and mass and therefore frequency encoding.

During the explosive period of mammalian radiation, two orders, Chiroptera (bats) and Cetacea (whales and dolphins), emerged with a wide range of highly evolved adaptations for arboreal and aquatic habitats, respectively, including hearing in radically different media. Two subdivisions of these orders, the suborder Microchiroptera (largely insectivorous microbats) and parvorder Odontoceti (toothed whales, dolphins, and porpoises), further evolved into echolocators with sophisticated biosonar systems for the production and analysis of ultrasonic signals and the returning echoes. For an echolocator, the key element is not simply the ability to hear and discriminate ultrasonic signals but rather the ability to produce an explicit signal that is tied to the objects of interest, either prey or obstacles, and to analyze returning echoes to decipher the presence, direction, and speed of targets of interest.

While we can find in some fossil specimens anatomical indicators of inner ears that were tuned to ultrasonic signals, we cannot be certain at what point in time the ability to echolocate occurred in any mammal. These changes in the skulls of bats and odontocetes occurred gradually and on different timelines. Bats were fully arboreal in the Eocene (56-34 MYA), whereas cetacean fossil skulls do not display clear evidence of telescoping until the Miocene (23-5 MYA) (Barnes et al., 1985). The emergence of exaggerated, complex pinnae and narial specializations such as nose leaves in bats and cranial alterations in dolphins are features in bat and dolphin evolution consistent with the onset of echolocation. For laryngeal echolocating microbats, a distinguishing characteristic is the unusual placement of the stylohyal bone connecting to the tympanic ring (Veselka et al., 2010). In toothed whales, there was a dramatic remodeling of the skull, termed "telescoping," referring to changes that relate to both life in water and the production and reception of underwater signals for echolocation. These include the migration of the narial bones dorsally to produce a "blowhole" for respiration, displacement of the frontal bones posteriorly, and elongation of the maxillae and mandibles, providing a hollow or scooped platform accommodating, in modern odontocetes, the fatty "melon" through which odontocetes emit outgoing echolocation signals.

For both groups, one driving force for biosonar may have been the absence of light. Microchiropteran bats are largely nocturnal, insectivorous predators. Odontocete cetaceans prey on fish, invertebrates, and aquatic mammals. They typically forage in daylight hours but hunt in deep or murky waters and therefore operate in essentially crepuscular conditions at best. Some species, such as the beaked whales, are capable of foraging as deep as 2,000 m with dives lasting over 2 h in lightless regions of the ocean (Tyack et al., 2006; Baird et al., 2008). Thus, while the primary target prey are quite different in size and behavior for bats and dolphins, and they operate in radically different habitats, they do share some environmental pressures that may have resulted in parallel evolution of echolocation, resulting in sophisticated biosonar systems and evident similarities in their ability to produce, detect, and analyze ultrasonic signals.

Because of the similarity of tasks and information that odontocetes and microchiropteran bats obtain acoustically from their environments, we expect that there are some commonalities in their auditory reception and processing mechanisms as well as differences related to alternative echolocation strategies and especially to media dependent elements reflected in the structure of their ears. These differences are manifested in differences in the structure and peak spectra of their echolocation signals, which in turn likely reflect wavelength and speed of sound in each medium, habitat and prey parameters, and spectral features of prime targets, all of which evolutionarily shaped hearing abilities. Further, there are niche and task dependent signal elements (Siemers and Schnitzler, 2004) and anatomical variations common to frequency-modulated (FM, short FM sweeps) and constant-frequency (CF-FM, long duration constant frequency tones followed by short FM sweeps) bats and mid vs. ultrahigh ultrasonic frequency odontocete ears (Pye, 1966; Ketten and Wartzok, 1990; Wartzok and Ketten, 1999; Fenton et al., 2012; Southall et al., 2019) that dictate critical feature extraction of echoes in air vs. water. Although there has been extensive research on the comparative anatomy of

mammalian ears, we still lack a precise understanding of how multiple anatomical variations observed across species affect hearing abilities.

The objective of the present study is to understand the similarities and differences of dolphin and bat inner ear morphometry related to the issues detailed above. Preliminary results from a smaller data set were published previously as an extended abstract in conference proceedings (Ketten et al., 2012). This paper provides the data for the first major stage in a research project focusing on similarities and differences of cochlear architecture and the implications for ultrasonic encoding and acuity amongst these groups. The primary goal is to put that data into a functional and comparative context. The key issues addressed are: (1) how do bat and dolphin ears differ from other terrestrial ears; (2) how do these differences correlate with air vs. underwater sound perception; and (3) what do the findings imply about the parallel evolution of adaptations for biosonar.

## SOUND IN AIR VS. WATER

In analyzing air vs. water borne sound adapted hearing, it is important to consider how the physical aspects of sound in each medium relates to acoustic cues. The following section summarizes key variables and their effect on measures of sound in air and water. For a comprehensive discussion see Urick (1983) and Rossing and Fletcher (2004).

In elastic media like air and water, "sound" is a disturbance that takes the form of acoustic waves. Basic measures of sound are speed, frequency, wavelength, and intensity. Because water is denser than air, sound in water travels faster and with less attenuation than sound in air. Sound speed in moist ambient surface air is approximately 340 m/s. Sound speed in sea water averages 1,530 m/s but will vary with any factor affecting density, such as salinity, temperature, and pressure. For each 1% increase in salinity, speed increases 1.5 m/s, for each 1°C decrease in temperature, 4 m/s, and for each 100 m depth, 1.8 m/s (Ingmanson and Wallace, 1973). Because these factors act synergistically, any marine, estuarine, or freshwater habitat has a variable sound profile that may change seasonally and with depth. For practical purposes, given in water sound speed is 4.5 times faster, and because frequency, measured in cycles/s or Hertz (Hz), is defined as the speed of sound (m/s) divided by the wavelength (m/cycle), the wavelength for any given frequency is 4.5 times greater than in air.

Concerning measures of hearing, intensity is a key feature, and its measures are dependent upon sound speed and arbitrary sound reference pressure. Sound intensity (I) is the acoustic power (P) impinging on a surface perpendicular to the direction of sound propagation, or power/unit area (I = P/a). In general terms, power is force times velocity (P = Fv). Pressure is force/unit area (p = F/a). Therefore, intensity can be rewritten as the product of sound pressure (p) and vibration velocity (v):

$$I = P/a = Fv/a = pv \quad (1)$$

For a traveling spherical wave, the velocity component becomes particle velocity (u), which can be defined in terms of effective sound pressure (p), the speed of sound in that medium (c), and the density of the medium ($\rho$):

$$u(x, t) = p/\rho c \quad (2)$$

We can then redefine intensity (2) for an instantaneous sound pressure for an outward traveling plane wave in terms of pressure, sound speed, and density (3):

$$I = pv = p(p/\rho c) = p^2/\rho c \quad (3)$$

The product $\rho c$ is the characteristic impedance of the medium. For air $c$ = 340 m/s and for sea water $c$ = 1,530 m/s. For air, $\rho$ = 1.29 kg/m$^3$ = 0.0013 g/cm$^3$; for sea water, density varies with temperature, salinity, and depth but on average, $\rho$ = 1,032 kg/m$^3$ = 1.03 g/cm$^3$. The following calculations show how these physical property differences for air vs. water influence intensity and sound pressure values:

$$I_{air} = p^2/(0.442\ g - m/s - cm^3) \quad (4)$$

$$I_{water} = p^2/(1575.9\ g - m/s - cm^3) \quad (5)$$

For a mammal to have an equivalent threshold in air and water requires the same acoustic power/unit area ($I_{air} = I_{water}$):

$$I_{air} = p_{air}{}^2/(0.442\ g - m/s - cm^3) = p_{water}{}^2/(1575.9\ g - m/s - cm^3) = I_{water}$$

$$p_{air}{}^2(3565.4) = p_{water}{}^2$$

$$p_{air}(59.7) = p_{water}$$

Therefore, the sound pressure in water must be ∼60 times that required in air to produce the same threshold response at the ear.

Because intensity (W/m$^2$) is difficult to measure, most studies of hearing thresholds rely on measures of sound pressure level (SPL) (see Au, 1993 for discussion). Sound pressure levels are expressed in decibels (dB) and are defined as:

$$dB\ SPL = 10 \log (p_m{}^2/p_r{}^2) = 20 \log (p_m/p_r) \quad (6)$$

where $p_m$ is the pressure measured and $p_r$ is an arbitrary reference pressure. However, there are different standardized reference pressures for SPL in air and water. For air-borne sound measures, the reference pressure is re 20 μPa. For underwater sound measures, the reference pressure is 1 μPa.

Consequently, for an ear with the same sound intensity threshold in air and water, the underwater sound pressure level would need to be 35.5 dB + 20 (log 20) dB greater than the airborne value. That is, a sound level measured as 61.5 dB re 1 μPa in water is equivalent to a sound measured as being 0 dB re 20 μPa in air.

These equations describe idealized and controlled measures of air and water borne sound. In comparing behavioral data from different species, particularly in comparing airborne and marine sound for mammalian hearing data, differences in experimental conditions are extremely important. We have no underwater equivalent of anechoic chambers, thus there are unavoidable ambient noise effects even in captive aquatic test conditions. In

addition, data for marine mammals are often available from very few individuals for which there may be no life history or prior hearing data and under test conditions that are highly variable particularly for studies on wild stranded animals. By combining research results from behavioral studies with biomechanical and anatomical studies, we obtain a more comprehensive picture of what and how each species hears and particularly how they hear in their respective habitats.

## MATERIALS AND METHODS

The ears from four species, two FM bats [the big brown bat *Eptesicus fuscus* ($n$ = 6) and the Japanese house bat *Pipistrellus abramus* ($n$ = 1)] and two odontocetes [the harbor porpoise *Phocoena phocoena* ($n$ = 6) and the bottlenose dolphin *Tursiops truncatus* ($n$ = 10)] were analyzed for this study (**Table 1**). Ears were examined using submillimeter imaging with two radiographic techniques, conventional helical computed tomography (CT) and microCT scanning using two analytical, fixed anode, rotating specimen scanners. All scans were performed on post mortem specimens of intact heads or extracted temporal bones.

### Specimens

The dolphin and porpoise heads and ears were obtained postmortem from male and female adult stranded animals under letters of authorization and USFW/NMFS permits (932-1489-08, 493-1848-00, 493-1848-02, 130062, and 130062-1) issued to DK. The specimens selected for study were relatively fresh material (postmortem condition designation Code 1 or 2) collected 1–24 h post mortem and with no evident auditory system pathology, such as intracochlear blood, evidence of torn or absent inner ear membranes or other cochlear partitions, necrotic middle ear mucosa, disarticulations of the ossicles, degenerate or absent auditory nerve, based on gross anatomical and CT examinations. The tissues were held chilled at 4°C until scanning. In the case of whole head specimens, post scanning, one or both temporal bones were extracted from each specimen, fixed in formalin by immersion and low pressure injection of formalin through the internal auditory canal and/or round window, and rescanned after 2 weeks or more to visualize any alterations in fixed compared to fresh tissue. Whole ears collected at the stranding site were held chilled and scanned the day of extraction, then processed as described above. Selected ears from these specimens were decalcified in EDTA and processed for transmission electron microscopy (TEM) or embedded in celloidin, stained with hematoxylin and eosin (H&E) or osmium tetroxide, and sectioned at 20 microns (for processing protocols see Schuknecht, 1953, 1993).

Adult big brown bats (four females, two males) were captured from attics and barns under permits issued by the State of Rhode Island, United States to JS. Because these animals were wild caught, the ages are unknown. The bats were housed in groups in the Brown University laboratory. All bats were in good health and echolocated normally during exercise and training. They were euthanized by intraperitoneal injection of Beuthanasia solution (0.03 ml). Heads were fixed in 4% paraformaldehyde and scanned in this solution. One additional bat was perfused with 0.9% saline followed by 4% paraformaldehyde. The head was placed in a decalcifying solution, embedded in paraffin, sectioned in the coronal plane at 5 μm thickness on a cryostat, and stained with trichrome. Use of animals was approved by the Brown University Institutional Animal Care and Use Committee and are consistent with United States federal regulations.

Japanese house bats were captured from a large colony living on bridge girders in Kyotanabe, Japan. They were brought to the laboratory and euthanized by intraperitoneal injection of sodium pentobarbital (65 mg/kg). Bat heads and extracted ears were fixed in 4% paraformaldehyde and scanned in this solution. Capture and use of these bats were approved by the Doshisha University Animal Experiment Committee and are consistent with Japanese law.

### Head and Ear Imaging

Heads and ears of all specimens were examined first using a Siemens Volume Zoom at the Woods Hole Oceanographic Institution Computerized Scanning and Imaging Facility[1]. The specimens were scanned using an imaging protocol of 0.5 mm acquisitions, 0.5 mm table speed. KV and effective mAS varied according to the mass of tissue being imaged. Data were acquired with an ultra-high resolution (U90 and U95 head) kernel, 200 FOV for whole heads. All helical CT images were produced with isotropic 100 micron voxels. Bone and soft tissue windows at standard and extended scales (see section "Middle Ear") were used for image reconstructions. All data and images were archived as both raw acquisition data and DICOM formatted image data files. Primary images were formatted at 0.1 mm slice thickness in the transaxial plane. Raw acquisition data were employed for imaging at smaller fields of view and for multiplanar reconstructions in sagittal and coronal planes and to digitally realign the slice plane to match a mid-modiolar cochlear axis.

[1]http://csi.whoi.edu

**TABLE 1** | Study specimens.

| Species | Common name | Ear specimens | Weight range (kg) | Average cochlear length (mm) | Standard deviation | Peak echolocation frequency (kHz) |
|---|---|---|---|---|---|---|
| *Phocoena phocoena* | Harbor porpoise | 6 | 55–78 | 25.6 | 1.42 | 100–110 |
| *Tursiops truncatus* | Bottlenose dolphin | 10 | 150–250 | 37.3 | 2.78 | 40–70 |
| *Eptesicus fuscus* | Big brown bat | 6 | 0.014–0.021 | 8.7 | 0.48 | 35–45 |
| *Pipistrellus abramus* | Japanese house bat | 1 | 0.005 | 6.8 | – | 43–52 |

For extracted ears, the same parameters were employed with images acquired at a 50 FOV. Each ear was scanned in a position approximating an *in situ* prone, anterior first position for the axial; i.e., short axis, cross-sectional slice images. This orientation typically gives the best initial approximation of a mid-modiolar cochlear projection.

MicroCT studies were performed on bat heads and extracted dolphin ears. Data were obtained first on an X-Tek MicroCT at the Harvard University Center for Nano Systems. For these studies, depending upon the dimensions and mass of the tissues, a Molybdenum or Tungsten anode was used with varying parameters for voltage and exposure times. The X-Tek uses a fixed head with a rotating specimen plate. For each study, 2,000–4,000 radial projection data were obtained and reformatted using VGStudio Max 2.0 into DICOM format into transaxial contiguous sections with an isotropic voxel of 11–40 microns. Additional data were obtained for bat specimens using a Zeiss Xradia Versa 520 at the Micro-CT and X-ray Microscopy Imaging Facility of Boston University. These data were acquired at 7–100 micron isotropic voxel resolutions and formatted by Zeiss platform software as DICOM images.

All image sets were further processed and reconstructed into 3D still and video images using Siemens proprietary VRT software, Amira 5.4, VG Studio Max 3.4, RadiAnt version 2020.1.1, software programs on 64-bit PC and Mac platforms.

## Cochlear Morphometrics

Cochlear canal midpoints and basilar membrane paths were identified based on membrane visualizations or, in their absence, on laminar positions from CT images for both the odontocete and microchiropteran ears to obtain Cartesian triplets (X, Y, Z) for three-dimensional (3-D) mapping, measurement, and reconstruction of the cochlear canal and basilar membrane path. Up to 30 mid-canal or membrane midline triplets, from the hook region (a recurved section at the most basal portion of the cochlear canal) to the helicotrema (the U-shaped section at the apex of the cochlear canal that connects scala media and scala tympani), were used to map each cochlea and measure spiral parameters (modiolar height and radii at each turn). For the odontocete specimens, measurements of the radii and of basilar membrane dimensions were obtained from mid-modiolar histology sections and by reslicing digitally 3-D reconstructions of the cochlea to produce radial slices along the spiral path. Parallel measures were made of the spiral from registered histology sets for the two odontocete species. These measurements were used to calculate cochlear and basilar membrane lengths with calculations based on the spiral parameters using the procedures and formulae described in detail in Ketten et al. (1998). These results were compared with cochlear length values obtained by measurement tools in the Amira software program. Basilar membrane thickness and width were obtained from specimens processed for transmission electron microscopy (TEM) ($n$ = 1 *T. truncatus* ear) and from histology sections stained with hematoxylin and eosin (H&E) ($n$ = 3 *P. phocoena*, 5 *T. truncatus* ears), with osmium tetroxide ($n$ = 1 *P. phocoena* ear), and with trichrome ($n$ = 1 *E. fuscus* ear). Ganglion cell counts and mapping were obtained from specimens in this study and from published data in prior studies as indicated in **Table 2**.

# RESULTS

Because of the stringent criteria for collection, postmortem condition, and checks on quality of tissues, particularly in the case of odontocete specimens, processing and analyses from the specimens in this study were completed over more than a decade. Some data on a few specimens have therefore been published previously, specifically those listed for ganglion cell counts (**Table 2**) and basilar membrane thickness and width (**Table 3** non-echolocating species). New data presented in this paper are found in **Table 1** for cochlear length averages and in **Table 3** for membrane and cochlear ratios in the species in bold. Additional new, important findings reported here are on variations in stapedial input and cochlear radii ratios and their functional significance.

## Auditory Bullae

While the tympanic and periotic bullae of the microchiropteran specimens analyzed are large in comparison to the total skull volume (see **Figure 1** and **Supplementary Video 1**), there are few differences in the actual bony structure, placement, and orientation compared to most mammals. The tympanic and periotic bullae in the bat are bulbous and are fused to the cranium. The periotic is positioned such that the apex of the cochlea points anteriorly with a slight ventral rotation (**Figures 1A,B**). This is a common orientation for land mammal inner ears. There is

**TABLE 2 |** Auditory and vestibular nerve densities.

| Species | Common name | Membrane length (mm) | Auditory ganglion cells | Density (cells/mm cochlea) | Vestibular ganglion cells |
|---|---|---|---|---|---|
| **Phocoena phocoena** | **Harbor porpoise** | **25.93** | **70,137** | **3117.20** | **3,200** |
| **Tursiops truncatus** | **Bottlenose dolphin** | **40.65** | **96,716** | **2486.27** | **3,489** |
| *Rhinolophus ferrumequinum* | Horseshoe bat | 16.1 | 15,953 | 991/1,750* | |
| *Pteronotus parnellii* | Mustached bat | 14.0 | 12,800 | 900/1,900* | |
| *Homo sapiens* | Human | 32.1 | 30,500 | 950 | 15,590 |

*Ganglion cell count data were compiled from this study (species in bold) and from previously published data by Bruns and Schmieszek (1980), Nadol (1988), Echteler et al. (1994), Gao and Zhou (1995), and Kössl and Vater (1995). *Densities at auditory fovea as described by Bruns and Schmieszek (1980). Ganglion cell counts for Phocoena and Tursiops are from histologies of the same specimens listed in **Table 3**.*

**TABLE 3 |** Cochlear morphometry of high and low frequency adapted cetacean and terrestrial mammals.

| Species | Common name | Total frequency range (kHz) | Turns | Basilar membrane length (mm) | Basal T/W (μm) | Apical T/W (μm) | Basal ratio (t/w) | Apical ratio (t/w) | Radii ratios |
|---|---|---|---|---|---|---|---|---|---|
| ***Phocoena phocoena*** | **Harbor porpoise** | **0.35–180** | **1.5** | **25.93** | **25/30** | **5/290** | **0.833** | **0.0172** | **3.62** |
| ***Tursiops truncatus*** | **Bottlenose dolphin** | **0.2–160** | **2.25** | **40.65** | **25/35** | **5/380** | **0.714** | **0.0132** | **4.39** |
| *Balaenoptera acutorostrata* | Minke whale | 0.02–30 | 2.25 | 50.6 | 11/130 | 3/920 | 0.085 | 0.00326 | 7.17 |
| *Balaenoptera musculus* | Blue whale | 0.01–18 | 2.25 | 71.0 | 7/120 | <2/2,200 | 0.058 | 0.0009 | 10.45 |
| *Elephas maximus* | Asian Elephant | <0.20–5.7 | 2.25 | 60.0 | –/– | –/– | – | – | 8.7 |
| *Felis domesticus* | Cat | 0.125–60 | 3.0 | 25.8 | 12/80 | 5/420 | 0.150 | 0.0119 | 5.71 |
| *Mus musculus* | Mouse | 5–60 | 2.0 | 6.8 | 15/40 | 1/160 | 0.363 | 0.0063 | 4.0 |
| *Rattus norvegicus* | Rat | 1–59 | 2.2 | 10.7 | 18/80 | 2/250 | 0.300 | 0.0106 | 4.3 |
| *Rhinolophus ferrumequinum* | Horseshoe bat | 7–90 | 3.25 | 16.1 | 35/80 | 2/150 | 0.438 | 0.0133 | – |
| ***Eptesicus fuscus**** | **Big brown bat** | **10–100** | **2.25** | **8.7** | **21/100** | **4/147** | **0.21** | **0.0272** | **3.4** |
| ***Pipistrellus abramus*** | **Japanese house bat** | **4–80** | **2.5** | **6.8** | | | | | **3.1** |

*Data in this table were obtained from specimens in this study (in bold) and from data published previously by Bruns and Schmieszek (1980), West (1985), Ketten and Wartzok (1990), Echteler et al. (1994), and Ketten (2000). Values for turns, radii ratios, and basilar membrane lengths were obtained from 3D reconstructions from CT scans and histology. Thickness and width of the basilar membrane (T/W) were measured by light microscopy from cochlear H&E histology sections for one bottlenose dolphin, one harbor porpoise, and one bat*. Therefore, membrane lengths differ from average lengths in* ***Table 1****. Hearing ranges are based on audiometric or electrophysiological data (Wartzok and Ketten, 1999; Surlykke and Moss, 2000; Boku et al., 2015; Southall et al., 2019) where available. Frequency ranges for the blue whale are based on vocalization data and for the minke whale, on vocalizations and FEM and cochlear frequency map models (Ketten and Mountain, 2011; Tubelli et al., 2012).*

**Data for basilar membrane dimensions for P. phocoena and T. truncatus specimens in this study were taken from radial sections located at 5–7% of cochlear length for the basal values and 98–100% for the apical values. These locations are consistent with locations for the remaining species except E. fuscus. E. fuscus data were taken from a paramodiolar section with basal values at a point approximately 20% of and 80% of length for the apex. The E. fuscus data are preliminary pending a full cochlear membrane morphometry map.*

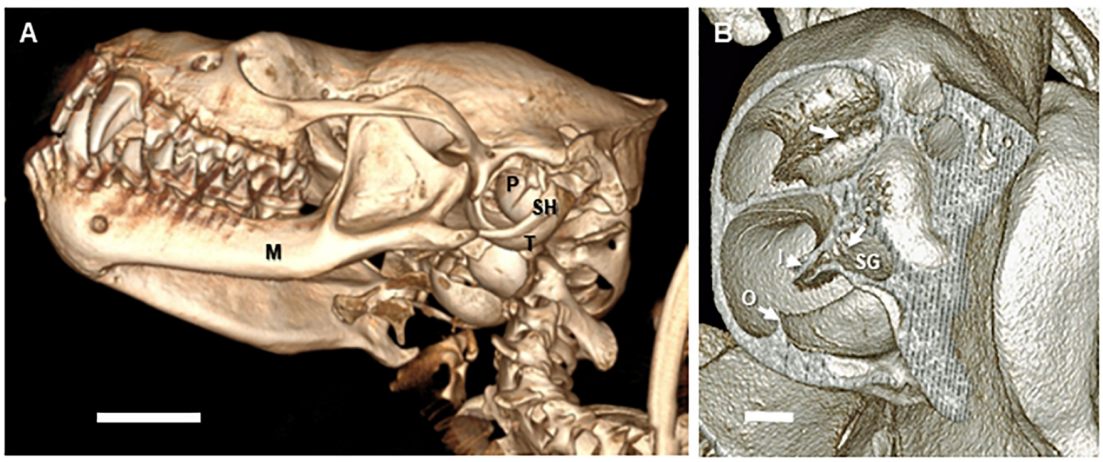


**FIGURE 1 |** Three-dimensional reconstructions of microCT images of the skull and auditory bullae of *Eptesicus fuscus* (big brown bat). The images are reconstructed from microCT data obtained at 11–17 micron voxel resolutions. **(A)** Left lateral view of skull of an adult female *E. fuscus* head. The manubrium of the malleus is visible inside the tympanic ring. M, mandible; P, left periotic bulla; SH, stylo-hyoid; T, tympanic bulla. Scale bar = 2.5 mm. **(B)** Dorso-lateral view of left cochlea in the same specimen. The wall of the periotic was removed digitally to reveal the mid to upper basal turns and laminae. Note the regular distribution of the foraminae of the habenula perforata (arrows) through which the afferent and efferent auditory (VIIIth) nerve fibers traverse the basilar membrane. I, inner osseous lamina; O, outer osseous laminae; SG, spiral ganglion (Rosenthal's canal). Scale bar = 0.1 mm. Images copyright 2020 DK, all rights reserved.

also in *E. fuscus* a well-developed, bony stylohyal flange that connects directly to the latero-posterior wall of the tympanic bulla (**Figure 1A**), consistent with bats that generate echolocation signals via the larynx (Veselka et al., 2010).

By contrast, the tympanic and periotic in the odontocetes in this study differ from the bat anatomy in location, orientation, and degree of attachment to the skull. The odontocete tympanic and periotic are connected to each other, forming a tympano-periotic complex, but are not fused to the skull (**Figures 2A,B**). The periotic is attached at its posterior margin to the tympanic (**Figures 2B,C**). The periotic which houses the cochlea and vestibular system is composed of exceptionally dense compact bone. The tympanic is hollow and distinctly cone shaped with a broad, thickened posterior and thin, friable body. This tympano-periotic complex is extra-cranial, suspended by ligaments in the peribullar fossa, ventral and posterior to the extended flange of the squamosal bone and just medial to the posterior edge of the mandibular ramus. The stylohyal bone

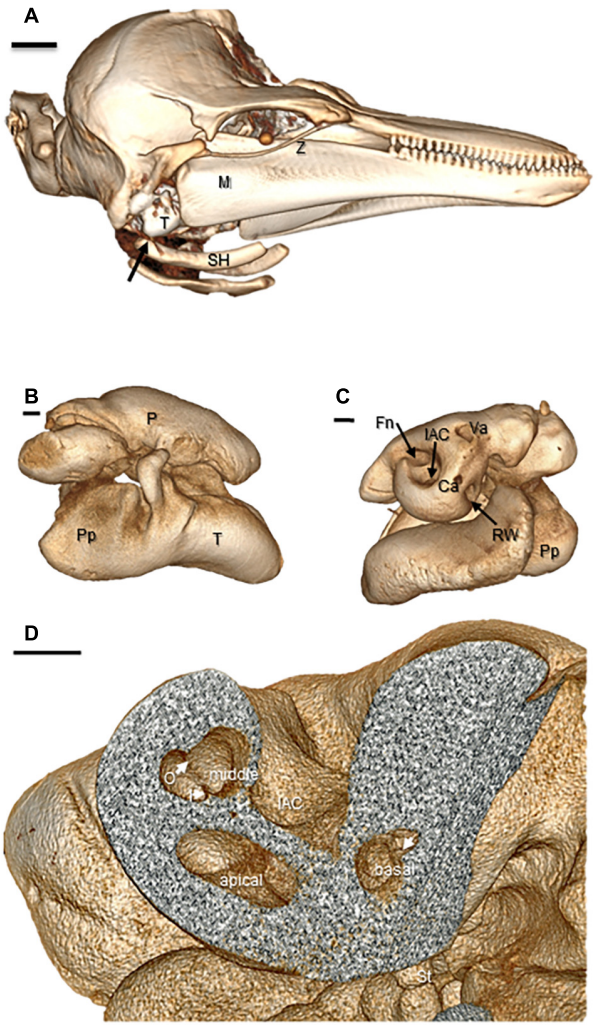


**FIGURE 2 |** Three-dimensional reconstructions of CT images of the entire head and auditory bullae of an adult male *Phocoena phocoena (harbor porpoise*). Ca, cochlear aqueduct; Fn, facial (VIIth) nerve canal; IAC, internal auditory canal of the acousto-vestibular (VIIIth) nerve; I, inner osseous lamina; M, mandible; O, outer osseous laminae; Pp, tympanic posterior prominence; P, periotic bulla; RW, round window; SH, stylohyal bone; St, stapes head; T, tympanic bulla; Va, vestibular aqueduct; Z, zygomatic (Images copyright© 2020 DK, all rights reserved). **(A)** Whole head image reconstructed from helical CT scan data with 1 mm slice acquisitions. Right lateral view of head shows the tympano-periotic complex in the peribullar fossa posterior to the mandible and associated stylohyal structures. Scale bar = 2.0 cm. **(B)** Lateral view of right tympano-periotic bullae images obtained from microCT with 500–1,500 projections and 33 micron voxel resolution. Scale bar = 2.0 mm. **(C)** Medial views of right ear tympano-periotic complex. Scale bar = 2.0 mm. **(D)** Cut-away of the periotic showing cochlear canal cross sections of the basal, middle, and apical turns with differences in spiral laminae separations (arrows) that reflect basilar membrane widths at each level. Scale bar = 2.0 mm.

(also referred to as stylo-hyoid) of odontocetes is well-developed but is connected to the tympanic typically by only a small ligament which attaches to a cartilaginous cap on the outer posterior prominence of the tympanic bone (**Figure 2A**). This suggests there is little or no transmission of laryngeal sound via the stylohyal bone in toothed whales and is consistent with ultrasonic signals generated via narial passages with "phonic lips" and nasal sacs; which are not found in baleen whales (Reidenberg and Laitman, 2018).

The whole complex is rotated medially 15–20°. The cochlear spiral within the periotic is oriented with the apex directed ventrally (**Figure 2C**). The acousto-vestibular (VIIIth) nerve projects inward from medial surface of the periotic, crossing the retro-peribullar space, to enter the temporal bone of the skulls; i.e., it is not enclosed in a bony internal auditory canal although it is encased in a heavy fibrous sheath. Species-specific variations in some of these features among odontocetes and particularly in comparison to the bullar and cochlear anatomies of mysticete (baleen) whales have been described in prior studies (see Reysenbach de Haan, 1956; Norris, 1969; Oelschlager, 1986; Ketten, 1992; Echteler et al., 1994; Nummela, 1995; Fordyce and de Muizon, 2001; Yamato et al., 2012).

## Middle Ear

Microchiropteran bats and odontocetes have similar features in their middle ears that enhance stiffness, including dense calcified middle ear ligaments, struts, and stiffer annular ligaments than most mammals. A new, notable feature of middle ears in both bat and odontocete specimens found in this study is that microchiropteran and odontocete ossicles, despite radical differences in size, have similar, exceptionally high Hounsfield values (HU) ranging 1,500–4,800. HU, named after the primary inventor of computed tomography, are dimensionless units that represent the summated relative attenuations at each detector for the multiple radiation beams transmitted in each transit of the radiation source. HU's are a representation of the measured attenuation coefficients of tissues or objects detected normalized to the density of air (−1,000) and water (0). The HU upper bound depends upon the scanning protocol and machine software. Standard clinical ranges are −1,000 to +3,071, and most animal tissues do not exceed +2,000 HU. Some systems are able to use "extended scales" developed primarily for imaging metallic implants, which provide HU values up to +44,000.

The ossicles and periotic capsules of the ears examined in this study commonly ranged over 3,000 HU compared to maxima of 1,000–1,200 for these structures in humans and most other mammals. HU are not a direct measure of density but they are interrelated, and these high HU values are consistent with exceptionally dense, stiff ossicular bones. HU values also indicate the tensor tympani is partially calcified, which was confirmed on histology. The stapedial muscle is disproportionately large compared to humans and cats, and the tympanic membrane and annular ligament are thick and relatively stiff; i.e., resisting manual movement of the stapes. This is consistent with nanoindentation studies (Miller et al., 2006) that showed *T. truncatus* and one bat species, *Rhinolophus ferrumequinum*, the horseshoe bat, to have acoustic stiffness values of $\sim 10^{17}$ Pa/m$^3$, which was two orders of magnitude greater than the majority of all other species in their study. Further, in both bat species in this study, there is a well-developed band of fibrous tissue, analogous to the stylo-hyoid ligaments

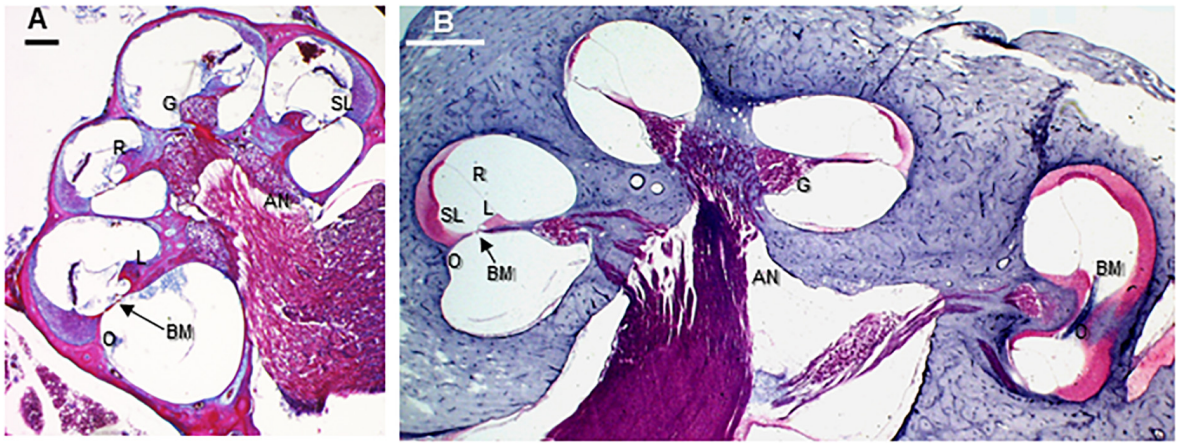


**FIGURE 3 |** Paramodiolar sections showing basal, middle, and apical turns in the big brown bat (*Eptesicus fuscus*) and harbor porpoise (*Phocoena phocoena*). AN, auditory nerve; BM, basilar membrane; G, ganglion cells; L, spiral limbus; O, outer spiral lamina; R, Reissner's membrane; SL, spiral ligament. Scale bars = 0.1 mm. **(A)** Big brown bat (*E. fuscus*) trichrome stained paramodiolar cross-section. **(B)** Harbor porpoise (*P. phocoena*) H&E stained midmodiolar section. The location of this section approximates the position of the microCT cross-section in **Figure 2D**. The basilar membrane is shown in an ascending longitudinal position in the hook region. The cochlea is inverted from the *in vivo* position to match conventional cochlear section image orientations. Images copyright© 2020 AS and DK, all rights reserved.

in other mammals and has been reported for other bat species (Veselka et al., 2010). This band joins the posterolateral edge of the bulla to the posterior margin of the mandible and stylo-basihyoid complex. As discussed in Veselka et al. (2010), these fibrous tissues may be important for coordinating vocalizations with auditory attention and receptivity.

## Cochlear Cytoarchitecture and Morphometry

Odontocete and microchiropteran cochleae have the prototypic mammalian divisions: scala media (cochlear duct), scala tympani, and scala vestibuli. The membranous labyrinth of the scalae form a spiral inside the bony labyrinth of the periotic, curving around a core, the modiolus, containing the auditory branch of the VIIIth nerve (**Figure 3**). Three anatomical features of the inner ear which influence resonance characteristics and frequency perception are addressed in detail here: basilar membrane construction and support specializations, spiral ganglion cell distributions, and cochlear spiral morphometry.

In all species examined in this study, the organ of Corti anatomy has the same basic cellular cohort as non-echolocating mammals but there are differences in the number, packing, cellular substructure of many features. Some structures of the scala media are hypertrophied, such as enlarged support cells, thickening of the basal basilar membrane primarily through increased collagen fiber density (**Figure 4**), and increased cellular density of the stria vascularis and spiral ligament (**Figures 3–5**). Similar features have been discussed in detail by a number of authors for some species of both dolphins (Wever et al., 1971a,b, 1972) and CF-FM bats (Vater, 2004).

Outer laminae in conjunction with the spiral ligament in most mammals buttress the basilar membrane, particularly those with high frequency hearing. The presence and extent of the outer laminae that hold the basilar membrane rigidly both laterally and medially varies by species. The specimens we examined had substantial outer osseous laminae running 20–60% of the basilar membrane length, varying by species. The thickness of the inner laminae varies inversely with distance from the stapes. The outer lamina in the basal end is as much as 40 μ in depth in *P. phocoena* (**Figures 4**, **5A**) and is heavily calcified (see **Figures 3–5** and **Supplementary Video 3**). MicroCT scans of *E. fuscus* (**Figure 1B**) indicate that similarly deep-layered laminae are present in that species as well. Further measurements of laminar thickness and percentage of cochlear length from histology for the bat specimens are in progress.

In mammals, basilar membrane thickness and width vary inversely from base to apex (von Békésy, 1960; West, 1985). Highest frequencies are encoded in the narrow, basal region; toward the apex, as the membrane broadens and thins, the membrane responds preferentially to progressively lower frequencies. Width and thickness change at different rates according to species in both land and marine animals (Ketten, 1992, 2000; Echteler et al., 1994). **Table 3** provides recent basilar membrane data for the specimens in this study from both CT and histology and compares findings in other mammals. Basal thickness and width ratios are similar in both the air and water echolocators, and are significantly different than in species with better lower frequency hearing. In the case of the porpoise, the basalmost membrane region was virtually a square cross-section as discussed below in more detail. The greatest differences across species in the membrane ratios were found in the apical regions. Estimations of basilar membrane width and thickness can be made from microCT, but require histologic preparations for accurate measurement. Data for basilar membrane dimensions for *P. phocoena* and *T, truncatus* specimens were taken from radial sections located at 5–7% of cochlear length in each specimen for basal values and 98–100%

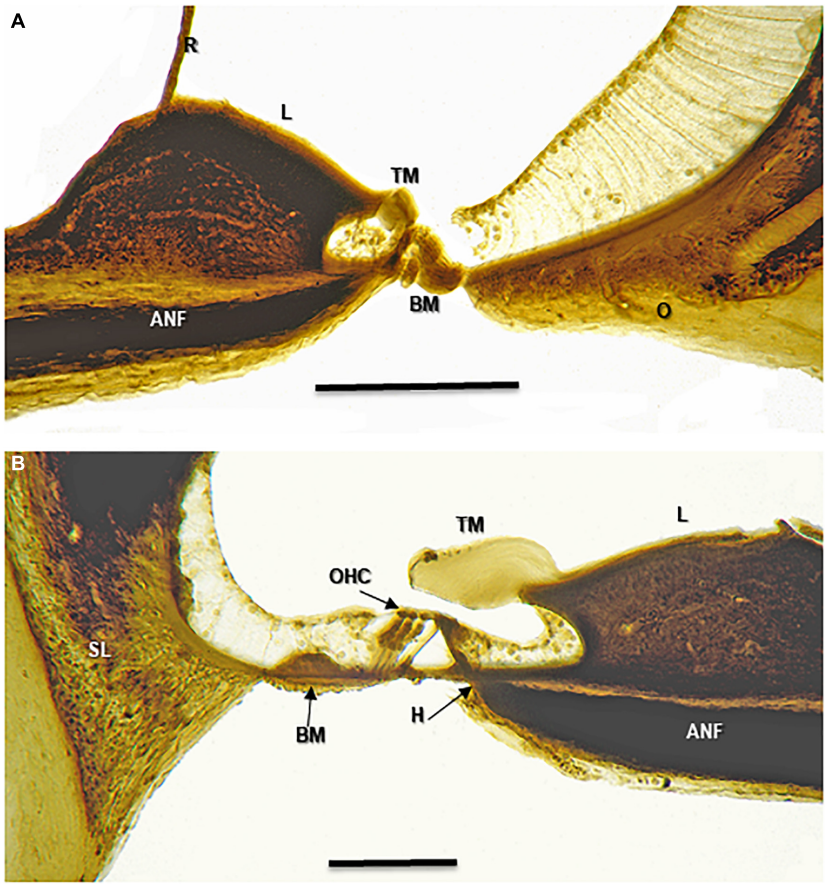


**FIGURE 4 |** Osmium tetroxide stained 25 micron sections of the of a harbor porpoise (*P. phocoena*) cochlea. These images should be compared with the TEM and schematic images in **Figure 5**. ANF, auditory nerve fiber; BM, basilar membrane; H, habenula; L, spiral limbus; O, outer spiral lamina; OHC, Outer hair cells; R, Reissner's membrane; SL, spiral ligament; TM, tectorial membrane. Scale bars = 0.1 mm. **(A)** Lower basal turn. **(B)** Mid apical turn. Images copyright© 2020 DK, all rights reserved.

for apical values, which are consistent with locations for the data for the other species except *E. fuscus*. The *E. fuscus* data were taken from a paramodiolar section with basal values at a point approximately 20% of length from the base and 80% length for the apex values. They are therefore not directly comparable to the other data in the table and are preliminary pending a full cochlear membrane morphometry map.

Total ganglion cell counts and ganglion cell densities measured from histologies of the odontocete specimens are given in **Table 2**. Average ganglion cell densities for the two odontocetes are more than twice those counted in the CF-FM horseshoe and mustached bats (Bruns and Schmieszek, 1980) and in humans (Nadol, 1988). They are also 30–50% greater than the highest densities reported in the basal, foveal regions in the two species of bats. Ganglion cell counts and distribution data are not yet available for bat species in this data.

## Three-Dimensional Anatomical Features

Reconstructions from microCT images coupled with the detailed histology of middle ear and cochlear features provided unexpected insights into peripheral auditory system architectures. **Figures 1**, **2** show images of the bullae; **Figures 3–5**, the cochlear duct; and **Figure 6**, the ossicles, the cochlear capsule, basilar membrane paths, and cochlear spiral variations. Videos revealing the exterior and interior cochlear topography and the relationship of the basilar membrane to stapedial locations in the sampled species are available in the **Supplementary Material**.

These reconstructions revealed unusual fenestral placements for the stapedial input to the cochlea compared to most mammals. The *Tursiops* specimens have a typical mammalian inner ear spiral configuration with the stapes located near the vestibule toward the base of hook region. However, in the other three species, the position of the stapedial input differs from this expected placement. In *E. fuscus* (**Figure 6A**) and *P. abramus* (**Figure 6B**), the oval window/stapedial footplate is located well above the vestibule and descending portion of the hook. This unusual placement was earlier observed in one *E. fuscus* ear (Ketten et al., 2012). We have now confirmed this placement in the ears of five additional big brown bats, both males and females. The *P. phocoena* cochlea (**Figures 6C,D**) exhibited the most extreme modification with the oval window located at the

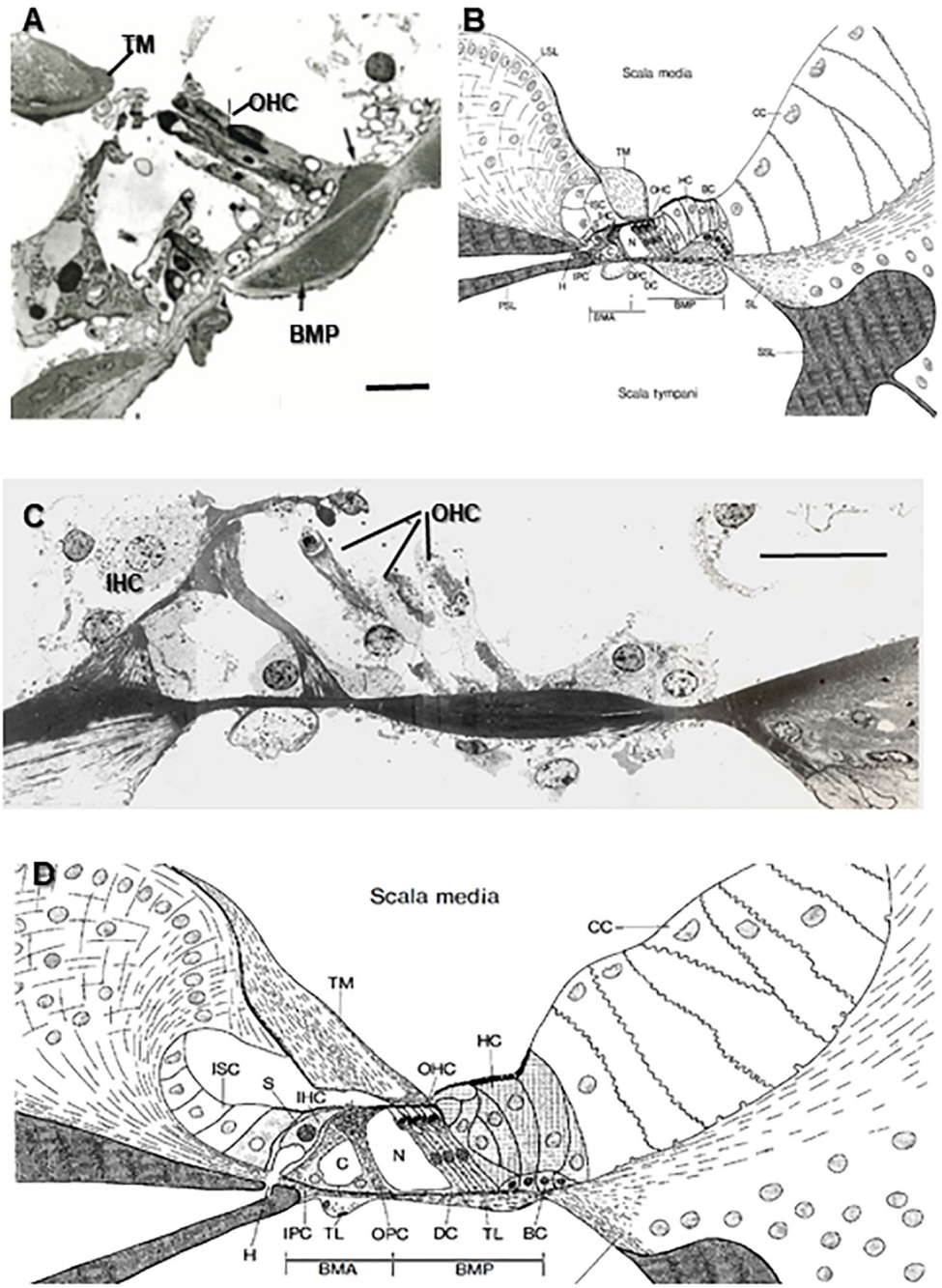


**FIGURE 5 |** Transmission electron microscopy (TEM) images of odontocete basilar membranes and organ of Corti compared with schematics of the cochlear sections from the horseshoe bat (*Rhinolophus ferrumequinum*). The specialized basal regions of the porpoise and bat have similar thickened regions of collagen fibers (arrows) attached to the basilar membrane that run longitudinally (scala media side) and transverse/radially (scala tympani side) that are hypothesized to act as stiffening agents. In both species, the outer hair cells (OHC) sit atop the bundle of longitudinal fibers. Specialized bundles are absent in the upper basal and second turn of the bottlenose dolphin and bat. Note: Because the OHC are actually staggered, all three may not be fully shown in the TEM images. This is not indicative of hair cell loss. BMA, Arcuate zone of the basilar membrane; BMP, Pectinate zone of the basilar membrane; C, Tunnel of Corti; CC, Claudius' cells; DC, Deiters' cells; H, Habenula; HC, Hensen's cells; IHC, Inner hair cells; IPC, Inner pillar cells; ISC, Inner sulcus cells; LSL, Limbus of the spiral lamina; N, Nuel's space; OHC, Outer hair cells; OPC, Outer pillar cells; PSL, Primary spiral lamina; S, IHC supporting cells; SL, Spiral ligament; SSL, Secondary spiral lamina; TL, Tympanic layer; TM, Tectorial membrane. Scale bars = 0.02 mm [TEM images copyright© 2021 DK, all rights reserved. Diagrams from Bruns (1980) reprinted by permission from Nature/Springer from Anatomy and Embryology, vol. 161]. **(A)** TEM image from the specially adapted lower basal half turn of a harbor porpoise (*P. phocoena*, 1200X magnification). **(B)** Schematic from Bruns (1980) of lower basal turn location in the horseshoe bat (right, *R. ferrumequinum*). **(C)** TEM image from the unspecialized region of the upper basal turn in a bottlenose dolphin (*T. truncatus* 2000X magnification). **(D)** Schematic of the basilar membrane and organ of Corti in a horseshoe bat (*R. ferrumequinum*) in the unspecialized upper second turn.

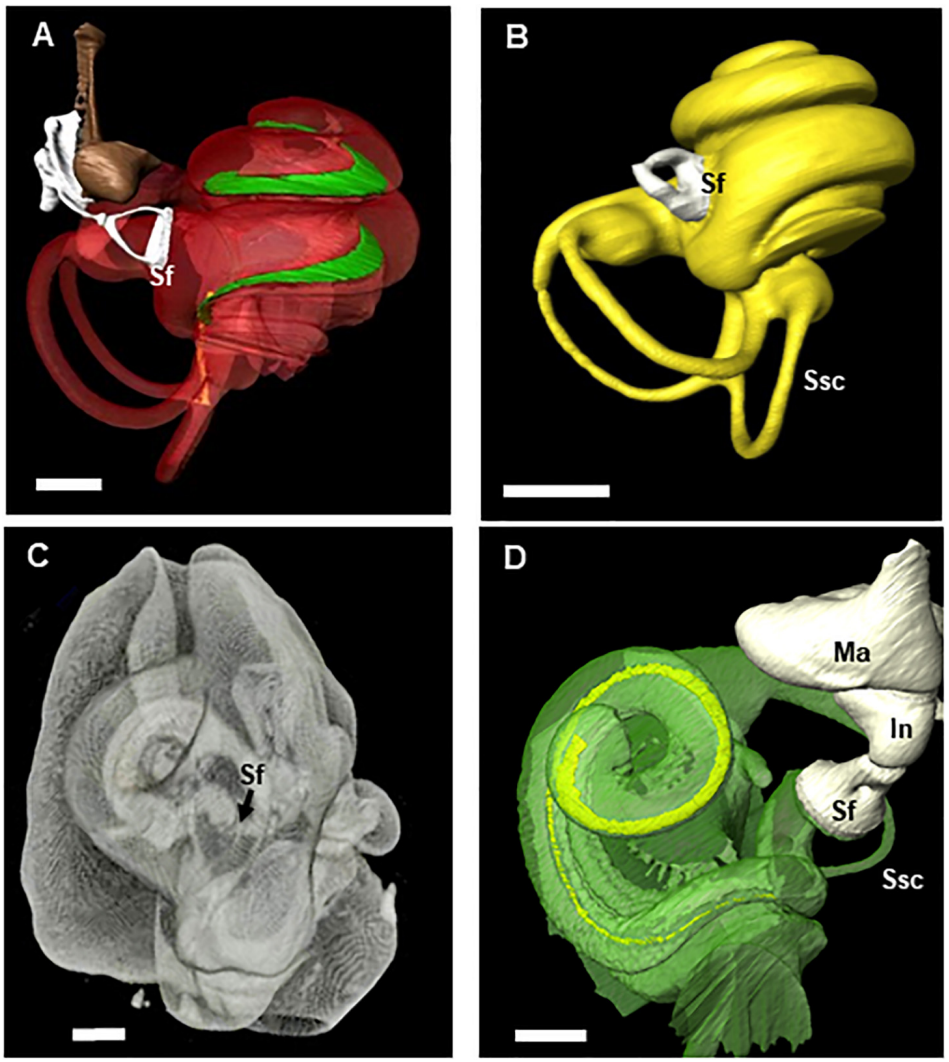


**FIGURE 6 |** 3D reconstruction from microCT scans of the middle ear ossicles and inner ears in two species of echolocators (big brown bat and harbor porpoise) with unusual stapes input positions. Videos (**Supplementary Videos 2, 3**) show rotations of the cochlear canals that become transparent to reveals the path and width changes of the basilar membrane from base to apex as well as the placement of the stapes and oval window in each of these species (images and multimedia copyright© 2021 DK, all rights reserved). Sf, stapes footplate; In, incus; Ma, malleus; Ssc, semi-circular canal. Scale bar = 1 mm. **(A)** *Eptesicus fuscus* (big brown bat). 3D reconstruction using Amira of a left ear obtained from 17 micron voxel X-Tek MicroCT scan data. The cochlea has 2.25 turns. The basilar membrane (green) length is 8.7 mm and has a post-hook basal turn stapedial input (Sf) (see **Supplementary Video 2** to view rotations and basilar membrane path within the cochlear capsule). **(B)** *Pipistrellus abramus* (Japanese house bat) 3D reconstruction of left ear obtained from 17 micron voxel X-Tek MicroCT scan data. The basilar membrane length is 6.8 mm with a post-hook lower basal turn stapedial input (Sf). **(C)** *Phocoena phocoena* (harbor porpoise) right ear is shown reconstructed with the periotic and cochlear walls transparent to reveal the basilar membrane (yellow) path and stapes located at end of an extended, double hook. The image was reconstructed from 100 micron voxel scans of the entire tympano-periotic complex within the head. The darkened line along the cochlear canal is the edge of the outer osseus lamina, but the basilar membrane itself cannot be fully resolved in this scan series. **(D)** This higher resolution image of a *Phocoena* cochlea was reconstructed from 18 micron voxel microCT scan data. The cochlea has 1.5 turns and basilar membrane length of 24.5 mm. In this species, a second arc rises from the first descending portion with the stapes footplate (Sf) located at its terminus (see **Supplementary Video 3** to view rotations and basilar membrane path within the cochlear capsule).

end of a second, reversed hook extending from the end of the primary descending basilar membrane hook region.

**Table 3** contains radii ratios for these cochleae. The ratio of the radii of curvature is defined as the radial length from the modiolus to the outermost length of the basal turn divided by the radius at the point of the helicotrema. It is an approximation of the curvature gradient (Manoussaki et al., 2008). The lower the value, the tighter the coiling. Equiangular curves, the broad based spirals with logarithmic increases in interturn distances that are most common in nature, therefore have larger ratios than Archimedean curves which have a constant interturn distance, as seen in a flat, tightly coiled rope.

The *T. truncatus* cochlear canal is a conventional equiangular curve common to most mammalian ears and has a radii ratio of 4.9. *E. fuscus* and *P. abramus* approximate Archimedean spirals and have ratios of 3.5 and 3.1, respectively. *Phocoena* has a ratio

of 4.3 and appears to be an Archimedean spiral but is difficult to categorize with certainty because it has only 1.5 turns. These ratios are in sharp contrast to the values for low frequency adapted ears, which typically range 8–12 in both land and aquatic species (**Table 3**; see also Manoussaki et al., 2008).

# DISCUSSION

## Air vs. Water: Matches and Misses

How well do the ears of echolocating mammals, in air or water, mesh with the general land mammal hearing scheme and how different or similar are microchiropteran and odontocete ears in this context of substantial differences in their natural habitats but common echolocation abilities?

In echolocation, or biosonar, the auditory system serves as a real-time sonar system that performs with greater versatility than man-made systems (Simmons, 2017). Identifying the auditory mechanisms responsible for superior performance is of great technological interest. The middle and inner ears of bats and toothed whales differ substantially with regard to mechanical coupling of sound from air or water to the middle and inner ear, or more specifically to the receptor array of the organ of Corti and the critical step of transducing acoustic parameters into neural inputs to higher auditory centers. By comparing the ears of aerial and aquatic echolocators we are beginning to explore this coupling to better understand how the auditory structures, their mechanics, and their respective environments result in similarly effective strategies for echolocation. Critically, several behavioral tests of biosonar performance show that big brown bats and bottlenose dolphins have perceptual acuity for echo delay and for the phase of biosonar echoes (Simmons et al., 1990; Finneran et al., 2020). For this to occur, both bat and dolphin auditory receptors, particularly the cochlea, must capture and convey fine echo delay and phase information via afferent signals to the auditory brainstem and temporal lobes, and be responsive to efferent control of peripheral responses in return. There are major differences in microchiropteran and odontocete ears related to air vs. underwater hearing, but the point in this sequence of reception, transduction, and processing where these differences fade and the functional anatomies converge is the cochlea. The goal of this on-going study is to describe this convergence to address how biosonar "works" and at the same time how it works in two very different acoustic realms.

Sensory systems evolved to allow animals to receive and process information from their surroundings but also to avoid overload (von Uexküll, 1957 translation, Wartzok and Ketten, 1999). In that sense, they are tuned to stimuli of greatest relevance, preferentially admitting some signals and incapable of receiving or processing others. Ears in all species act as highly selective, tuned filters, selecting and attending to signals that, evolutionarily, proved to be important in the context of their local environment (Ketten, 1992). Most animals, including whales and dolphins (Ketten and Wartzok, 1990), have vocalizations linked to their peak hearing sensitivities in order to maximize conspecific communication but also hear beyond their peak range to detect acoustic cues from predators, prey, or significant environmental cues. Further, hearing evolved in the context of natural ambient noise, which varies significantly by habitat. Wenz (1962) laid the ground work for assessing marine ambient noise and showed that it is dominated by frequencies below 5 kHz. Recently, growing concern for sound impacts has led to extensive efforts globally to assess the acoustic environment of diverse habitats, both at sea and on land. These studies have shown that even relatively small contiguous areas can vary significantly based on landscape and vegetation differences (Slabbekoorn, 2004).

Both bats and whales evolved from land-dwelling ancestors during the explosive period of mammalian radiation. Bats of course continued to evolve in air, while the archeocetes moved into aquatic habitats but retained the essentials of air-adapted ears; e.g., an air-filled middle ear and spiral cochlea (see Barnes et al., 1985; Fordyce and de Muizon, 2001; Ekdale, 2016). Therefore, some similarities in land and aquatic mammal hearing anatomy mechanisms are not surprising. For microchiropterans and odontocetes, however, the most striking similarities are not the basic mammalian ear components but rather the specializations or modifications that link to ultrasonic hearing and echolocation abilities.

Land and marine ears, and specifically bat and dolphin ears, do have considerable structural differences. The majority of those differences are in the structure of the reception pathways and the locations of the ears rather than in the middle and inner ear anatomy. As marine mammal ancestors became more aquatic, air-adapted mammalian ears had to not only be coupled to water-borne sound but also adapted to an ambient sound field dominated by low frequencies for hearing to remain functional.

Ear evolution in cetaceans took place in tandem with, and in part in response to, body reconfigurations. Just as the physical demands of operating in water exacted a structural price in the locomotory and thermoregulatory systems of whales, physical differences in underwater sound required some auditory system remodeling. As the rostrum elongated, the cranial vault foreshortened, and the nares and narial passages were pulled rearward to a dorsal position behind the eyes. Many conventional land mammal auditory components, like external pinnae and air-filled external canals were lost or reduced and the middle and inner ears migrated outward (Ketten, 1992, 2000). In most odontocetes, the ears have no substantial bony association with the skull. Instead, they are extra-cranial, suspended by ligaments in a foam-filled fossa outside the skull. In addition, there are specialized fatty bundles with distinct and unique lipid profiles in all odontocetes that parallel the mandible, connecting the middle ear, that have a discrete shape resembling elongated pinnae (Ketten, 1997, 2000; Koopman et al., 2006).

Several factors related to the physical characteristics of sound in water, such as speed, frequency of echolocation signals vs. target object size, drove the specializations of the auditory system in odontocetes. The speed of sound in water drove cetacean ears to be farther apart compared to other mammals; new sound reception pathways matched to acoustic impedance characteristics of water developed, and acoustic isolation of outgoing signals from the ear was achieved by ears that are uncoupled from the skull, given the five-fold increased speed of sound in water, the almost cartoonish large cetacean heads and

extracranial ear placements provide odontocetes with interaural time difference discriminations comparable to that of bats.

Since bats evolved and remained in air, acoustic properties of the media were not so evident a factor for major retooling of the auditory periphery although there are clear anatomical specializations for flight. In one sense, they can be seen as enhancing or honing rather than reshaping their auditory systems. The complex and relatively delicate structures of the pinnae and nose leaves in some species are as striking and intriguing as telescoping and specialized fats in odontocetes. All of these features require more extensive biomechanical analyses as well as the related questions of if and how bats deal with air flow noise in flight and dolphins deal with water flow noise in dives to reduce interference with echo perception.

The most striking and functionally significant observations related to the specimens in this study, and the observations that set them apart from the majority of mammalian ears, are in fact their similarities, particularly the augmentations observed in the middle ear ossicular stiffening and control structures in the middle ear, the unusual stapedial locations for three of the studied species, the basilar membrane foveal membrane regions in one species, and the increased ganglion cell densities compared to other mammals. Our data on ganglion cell counts are preliminary at this time, and it is important to clarify whether the location of high ganglion cell densities coincide with frequency place maps for the peak spectral characteristics of echoes in each group.

The intracochlear distribution of the outer lamina expressed as a percentage of membrane or cochlear ranges from 20% in *Tursiops* to over 60% in *Phocoena*. The data from microCT images suggest that the bat distributions are similar. Extensive buttressing is consistent with higher resonant frequencies as well as less potential variability from more elastic suspension systems. Fleischer (1976) observed that osseous laminae may have material properties in the basal region comparable to solid compact bone and decreasing apically as fibrous inclusions increase, producing a potential 100-fold to 1,000-fold base to apex stability gradient. If correct, these values suggest that differences in laminar support may be a far more influential element of basilar membrane dynamics than is currently understood. They also underscore that material property measurements on a species basis should be prioritized to aid accuracy in Finite Element Models (FEM) of tissues in both the middle and inner ear (Tubelli and Ketten, 2019; Puria, 2020).

Within the inner ear of all cetaceans, one major dissimilarity from bats and in fact other mammals as well is the differences in vestibular dimensions. Not only is the vestibular system smaller in proportion to the cochlea, it is relatively poorly innervated (Gao and Zhou, 1995). Most mammals, including bats, have approximately 40–45% of the VIIIth nerve fibers distributed to the vestibular branch. In cetaceans, vestibular branch commonly has less than 7% of the total VIIIth nerve fibers. A number of features have been examined with regards to this question, including the possibility that the fusion of the cervical vertebrae affected inputs to the vestibular system, the velocity and frequency of rotations compared to land mammals, and the kinematics of cetacean swimming (Gingerich et al., 1994; Fish, 1998; Spoor et al., 2002; Kandel and Hullar, 2010). Nevertheless, the primary driver for this state remains unclear. Both bats and dolphins make fast and frequent re-orientations while seeking prey and avoiding obstacles. Therefore, they are subject to similar stresses on the vestibular system. That suggests that reduction of the vestibular system in cetaceans is not driven by their manoeuvers. This remains an open question.

## It's a Material World

The basilar membrane is a frequency-dispersing array that shunts a succession of frequencies from high to low to different locations, and thus to different receptors, creating frequency tuned channels for subsequent auditory processing (Dallos, 1996). Variations in rate of change in basilar membrane dimensions are consistent with differences in the octave ranges of hearing in each species, with gradations in thickness and width a reasonable proxy of the material properties of stiffness and mass. Consistent with the data in our study, Pye (1966) reported for the basilar membrane of another FM bat, *Pipistrellus pipistrellus*, a basal width of 80 μ with a thickness of 15 μ and an apical width of 115 μ with a thickness of 5 μ or less. If *P. abramus* is similar that suggests a basal membrane ratio of approximately 0.19 and apical of 0.04, which is similar to the preliminary values for *E. fuscus*. Although the membrane data are incomplete for the microchiropteran bats examined in this study, the preliminary data from histology for *E. fuscus* and microCT for *P. abramus* suggest they have smaller gradations in both thickness and width, changing little over the full cochlear length. This implies a narrower hearing range, with much higher low frequency and lower high frequency cut-offs compared to the odontocetes. Our data for these two bat species are consistent with those in CF-FM bats (reviewed by Echteler et al., 1994; Kössl and Vater, 1995). Of the two odontocetes studied, a full length basilar membrane morphometric maps of *P. phocoena* show markedly less gradation than *T. truncatus* and more closely resembles the *R. ferrumequinum* membrane gradient in its basal regions (Ketten and Wartzok, 1990).

Based on the anatomy of the basilar membrane in *P. phocoena*, specialist ears exist in both odontocetes and microchiropterans. *P. phocoena* has a basal cochlear membrane structure consistent with a specialized basilar membrane "foveal" region in the lower basal turn, similar to that reported for the CF-FM bat *R. ferrumequinum* (Bruns, 1980). The harbor porpoise basilar membrane has a thickened region with fairly constant width and thickness over a substantial portion of the basal basilar membrane (**Figures 4**, **5**). There are also longitudinal and transverse or radial fibers present, again paralleling those reported for *R. ferrumequinum*. These areas, dubbed "acoustic fovea" regions by Bruns (1980) and Bruns and Schmieszek (1980) are singularly devoted to frequencies near the peak spectra of their echolocation signals (100–110 kHz for the porpoise, 80–86 kHz for the CF-FM bat) and thus represent a stretched frequency map that occupies much of the basal turn of the cochlea modeled by Ketten (1994) which was later confirmed behaviorally by Kastelein et al. (2002).

There are, however, additional elements evident in these ears, including the inner and outer osseous laminae, that may have a significant role in determining responsivity, particularly for the upper limits of the hearing range by increasing the stiffness of the basilar membrane along its extent. These stiffening features

are part of the reason that the basilar membrane of *P. phocoena* has a peak sensitivity of approximately 110 kHz and extends to nearly 200 kHz (Kastelein et al., 2002), despite having a cochlear length equivalent to a cat (Greenwood, 1990). Were the *P. phocoena* frequency map derived from a single parameter, such as length, the hearing range would have been substantially lower with a cut-off near 60 kHz rather than the 180–200 kHz estimated in more complex models (Ketten, 1994; Ketten et al., 1998). This is because length is correlated with body mass. Calculations of frequency ranges and cochlear maps based solely on a single parameter such as cochlear length or number of turns are less definitive than multi-parametric estimations and are generally not reliable for species operating in different media with radically different constraints on body mass. Bats and dolphins as two extreme examples of this underscore the importance of considering multiple facets of the functional anatomy of the ear in making comparisons across species.

## Waves

The most common model of intracochlear acoustic propagation is that the majority of the cochlea may have some response to introduced sound stimuli, but depending upon its properties and those of each membrane region the amount of deflection and phase of the signal will vary. The progressive phase and amplitude variations have been described as a traveling wave that produces a time dependent response "envelope" of amplitudes that characterizes the signal (Dallos, 1996).

Could species variations in location of the oval windows with respect to the basilar membrane segments suggest alternative response mechanisms? Simulation experiments (A. Hubbard, pers. comm.) indicate that changing response parameters to constant tuning from 20 to 40% resulted in a standing wave. In big brown bats, the exceptional position of the oval window opens several possibilities, including bi-directional flow propagation and resultant reflection effects that may also produce a localized standing wave phenomenon.

The concept of a standing wave has been proposed previously in relation to the acoustic fovea of CF-FM bats (Kössl and Vater, 1995). These authors proposed that the relative thickening of the basilar membrane could provide a reflection zone tuned to returning echoes. This hypothesis also would function to enhance Doppler detection. In this paper, we have presented another potential mechanism for standing wave generation in *E. fuscus,* a species not known to have an acoustic fovea. Our hypothesis is not in opposition to that put forward by Kössl and Vater. Rather, it may be an alternative means to a similar end for some species, and both have yet to be proven.

Thus far, among odontocetes, only the harbor porpoise has been shown to have basilar membrane characteristics similar to acoustic foveal regions in Microchiropterans. There is also no evidence to date that dolphins or porpoises use Doppler shift compensations. Indeed, Au (1993) concluded that sound speeds in water may produce sufficient repeat echoes over a short period of time to diminish the information that Doppler shifts may provide to dolphins about target prey velocity and direction. *Tursiops*, however, does not have the structural features that were found in *Phocoena.* Were Doppler sensitivity to be explored in any odontocete, or in fact other bats, it may be important to take cochlear anatomy into account.

## Spiraling Down

Radii ratios have been proposed as a correlate of low frequency hearing cut-offs (Manoussaki et al., 2008) based on the assumption that larger ratios reflect a broader curvature that would produce a "whispering gallery" effect in which energy density paths focus at the points of concavity, producing a radial pressure gradient. This is a favorable structure for low frequency energy to propagate throughout the cochlea. The compact spiral structure encountered in the FM bats in this study imply a decrease in the propagation for lower frequencies. Even more interesting is the additional reverse curve present in the harbor porpoise which suggests an alternative but potentially equally or more effective anatomical strategy for preventing low frequencies from penetrating the cochlea. This is in turn brings up the question of whether echolocators have developed structural measures to minimize exposure to spurious signals, such as low frequencies which dominate the marine environment.

## Potential Protection From Echolocation Adaptations?

Dolphin ears are essentially terrestrial ears immersed in a biologically rich but in other ways a harsh environment. Anatomically, they follow the basic land mammal pattern but they have extensive adaptations that accommodate substantial parasite loads, pressure changes, and concussive forces. It remains unclear whether the relatively noisy and literally high pressure oceanic environment led to ears more stressed by multiple impacts or the development of physiologically tougher than average ears (Maison and Liberman, 2000). On the other hand, because marine mammals evolved in a high noise environment and have adaptations that prevent structural ear damage from barotrauma, it is possible that this is a feature related to echolocation *per se*, similar to what has been hypothesized for bats. Simmons et al. (2016, 2017, 2018) found that hearing sensitivity of big brown bats is not impaired by long duration, high-intensity exposures to sounds at levels that are known to induce temporary threshold shifts in other mammals. Therefore, it may be that successful echolocators have one or more ways by which they are able to sustain hearing in the presence of their own repetitive and intense signals with the secondary benefit of being less subject to environmental noise and hearing deficits.

Cochlear microphonic studies on several species of bats have demonstrated that contractions of the stapedius are coincident with the onset of the out-going signal followed by a release, thus synchronizing signal-echo sequences (Henson, 1965; Suga and Jen, 1975; Kick and Simmons, 1984). In these experiments, attenuations of the initial signal ranged from 20 to 28 dB. These levels are consistent with attenuations in humans and other species for stapedial reflexes, but the key features that differentiate this ability in bats from a simple stapedial reflex to an intense sound is the closely timed synchronization with the emitted signal, its rapidity, and the sustainability of the

sequences. Studies have indicated an ability in several odontocete species, including *Tursiops* and *Phocoena*, to "self-mitigate" effects of exposure to loud underwater sounds in captive studies (Finneran, 2018; Nachtigall et al., 2018; Kastelein et al., 2020), the precise mechanisms of which remain unexplained.

## CONCLUSION

Cross-media commonalities suggest similar cochlear specializations developed in parallel in microchiropterans and odontocetes. Cochlear anatomy observed in all specimen groups are linked to peak spectra of their vocalizations, notably with expanded frequency representation in the inner ear and, in some cases, possibly with enhanced tuning hypothesized to be derived from standing wave phenomena.

Differences that are consistent with processing of aerial vs. aquatic borne sound are found primarily in the outer and middle ear elements. Other differences among species, such as peak frequency of echolocation signals, are correlated with signal type, prey, and/or habitat features.

One speculation is that the stapedial placements and uniform, robust basilar membrane structure may enhance tuning in adjacent ear segments by generating standing wave phenomena. In the FM bats, the stapedial locus may result in a bi-directional flow. In the phocoenids, the double hook may serve to attenuate low frequency penetration and thus reduce low frequency sensitivity providing more membrane space for a stretched response map. Delphinid odontocetes, represented by the bottlenose dolphin in this study, more closely resemble the terrestrial generalist ear, with a peri-vestibular input. In all species examined, the cochlear canal curvatures are consistent with those of the highest frequency terrestrial species.

## DATA AVAILABILITY STATEMENT

The raw data supporting the conclusions of this article will be made available by the authors, without undue reservation.

## ETHICS STATEMENT

Bat studies were reviewed and approved by the Brown University Institutional Animal Care and Use Committee; odontocete studies were approved by the IACUC committee of Woods Hole Oceanographic and collected under USFW/NMFS permits (932-1489-08, 493-1848-00, 493-1848-02, 130062, and 130062-1).

## AUTHOR CONTRIBUTIONS

DK collected all odontocete specimens and provided the histology and analyses of all data on odontocetes, conducted and analyzed CT scans of all specimens in the study, and wrote the primary draft of the manuscript. JS, HR, and AS provided bat specimens. JS and AS provided histological data for the big brown bat. All authors contributed to the interpretation of the data and edited the manuscript.

## FUNDING

MicroCT scanning, data analyses, and manuscript preparation were assisted by funding to DK from the Joint Industry Program (contract JIP22 III-16-08 – 55205300) and fellowships from the Hanse-Wissenschaftskolleg ICBM Fellowship and the Helmholtz International Fellow research programs. Big brown bat data collection and analysis were supported by an Office of Naval Research grant N00014-14-1-05880 to JS and an Office of Naval Research MURI grant N00014-17-1-2736 to JS and AS. Specimen collection, histology processing, and helical scanning related to the data reported in this study were supported through multiple grants and contracts since 2010 to DK from NIH, N45/LMRS-United States Navy Environmental Division (EnvDiv), Office of Naval Research, and ONR Global.

## ACKNOWLEDGMENTS

We are very grateful to the reviewers of this manuscript for their thoughtful comments and helpful suggestions which greatly improved the text. They particularly assisted with understanding what portions needed additional clarification or background. Extensive technological assistance was provided for helical scanning by Scott Cramer and Julie Arruda of Woods Hole Oceanographic Institution, and histology processing of tissues was provided by Jennifer O'Malley, Diane DeLeo Jones, and Barbara Burgess of Massachusetts Eye and Ear Infirmary. MicroCT images were obtained with the assistance of Aaron Nakasone at the Micro-CT and X-ray Microscopy Imaging Facility of Boston University. We thank Katie Moore, Misty Niemeyer, and Jennifer Skidmore for their assistance in obtaining specimens and the permitting processes as well as the volunteers of the Marine Mammal Health and Stranding Response Program, the International Fund for Animal Welfare (IFAW), and the National Oceanic and Atmospheric Administration, without which this research would not have been possible.

## SUPPLEMENTARY MATERIAL

The Supplementary Material for this article can be found online at: https://www.frontiersin.org/articles/10.3389/fevo.2021.661216/full#supplementary-material

**Supplementary Video 1 |** The data for the video were obtained from images reconstructed in RadiAnt version 2020.1.1 from microCT data obtained at 11–17 micron voxel resolutions on a Zeiss Xradia Versa 520. The video shows a digital dissection of a the head of a female bat (*Eptesicus fuscus*) from the exterior surface to the inner ear that progressively reveals the tympano-periotic complex, middle ear, and inner ear labyrinth. The head is shown first in anterior view. As the head rotates to the left side, the skin and soft tissues fade from view to reveal the skull of the bat. The middle ear structures, particularly the spike-like long arm of the malleus, are clearly visible inside tympanic ring, just posterior to the mandible. The video then focuses on these structures, removing the surrounding skull structures, and rotates the bulla from a lateral to anterior view, revealing the three ossicles and the semicircular canals of the vestibular system. The stapes can be seen situated at the basal turn of the cochlea as the bony cochlear capsule fades

to show the 2.25 turn spiral of the cochlea (see **Figure 1** for labeling of structures. Images and multimedia copyright© 2021 DK, all rights reserved).

**Supplementary Video 2 |** The data for the video were obtained from images produced in Amira from VG Studio Max 3.4 images reconstructions of 7–11 micron voxel acquisitions of microCT data obtained with an X-Tek MicroCT. The video shows the inner ear anatomy of a male bat (*Eptesicus fuscus*) first as the full periotic capsule (red) with the stapes (white), incus (white), and malleus in place. The capsule fades as the inner ear rotates, revealing the path and profile of the basilar membrane (green) within inner ear labyrinth (see **Figure 6** for dimensions and detail of the structures).

**Supplementary Video 3 |** The data for the video were obtained from images produced in Amira from VG Studio Max 3.4 images reconstructions of 18–25 micron voxel acquisitions of microCT data obtained with an X-Tek MicroCT. The images were processed for video using Osirix 12.0.

## REFERENCES


Au, W. W. L. (1993). *The Sonar of Dolphins*. New York, NY: Springer.

Baird, R. W., Webster, D. L., Schorr, G. S., McSweeney, D. J., and Barlow, J. (2008). Diel variation in beaked whale diving behavior. *Mar. Mamm. Sci.* 24, 630–642. doi: 10.1111/j.1748-7692.2008.00211.x

Barnes, L. G., Domning, D. P., and Ray, C. E. (1985). Status of studies on fossil marine mammals. *Mar. Mamm. Sci.* 1, 15–53. doi: 10.1111/j.1748-7692.1985.tb00530.x

Boku, S., Riquimaroux, H., Simmons, A. M., and Simmons, J. A. (2015). Auditory brainstem response of the Japanese house bat (*Pipistrellus abramus*). *J. Acoust. Soc. Am.* 137, 1063–1068. doi: 10.1121/1.4908212

Bruns, V. (1980). Basilar membrane and its anchoring system in the cochlea of the greater horseshoe bat. *Anat. Embryol. (Berl)* 161, 29–50. doi: 10.1007/BF00304667

Bruns, V., and Schmieszek, E. (1980). Cochlear innervation in the greater horseshoe bat: demonstration of an acoustic fovea. *Hear. Res.* 3, 27–43. doi: 10.1016/0378-5955(80)90006-4

Dallos, P. (1996). "Overview: cochlear neurobiology," in *The Cochlea. Springer Handbook of Auditory Research 8*, eds P. Dallos, A. N. Popper, and R. R. Fay (New York, NY: Springer), 1–43. doi: 10.1007/978-1-4612-0757-3_1

Echteler, S. M., Popper, A. N., and Fay, R. R. (1994). "Structure of the mammalian cochlea," in *Comparative Hearing: Mammals*, eds R. R. Fay and A. N. Popper (New York, NY: Springer), 134–171.

Ekdale, E. G. (2016). Form and function of the mammalian inner ear. *J. Anat.* 228, 324–337. doi: 10.1111/joa.12308

Fay, R. R. (1988). *Hearing in Vertebrates: A Psychophysics Handbook*. Winnetka, IL: Hill-Fay Associates.

Fenton, M. B., Faure, P. A., and Ratcliffe, J. R. (2012). Evolution of high duty cycle echolocation in bats. *J. Exp. Biol.* 215, 2935–2944. doi: 10.1242/jeb.073171

Finneran, J. J. (2018). Conditioned attenuation of auditory brainstem responses in dolphins warned of an intense noise exposure: Temporal and spectral patterns. *J. Acoust. Soc. Am.* 143:795. doi: 10.1121/1.5022784

Finneran, J. J., Jones, R., Guazzo, R. A., Strahan, M. G., Mulsow, J., Houser, D. S., et al. (2020). Dolphin echo-delay resolution measured with a jittered-echo paradigm. *J. Acoust. Soc. Am* 148:374. doi: 10.1121/10.0001604

Fish, F. (1998). Comparative kinematics and hydrodynamics of odontocete cetaceans: morphological and ecological correlates with swimming performance. *J. Exp. Biol.* 201, 2867–2877. doi: 10.1242/jeb.201.20.2867

Fleischer, G. (1976). Hearing in extinct cetaceans as determined by cochlear structure. *Jour. Paleon.* 50, 133–152.

Fordyce, R. E., and de Muizon, C. (2001). "Evolutionary history of cetaceans: a review," in *Secondary Adaptation to Life in the Water*, eds J. M. Mazin and V. de Buffrenil (Munich: Pfeil Verlag), 169–233.

Gao, G., and Zhou, K. (1995). "Fiber analysis of the vestibular nerve of small cetaceans," in *Sensory Systems of Aquatic Mammals*, eds R. A. Kastelein, J. A. Thomas, and P. E. Nachtigall (Woerden: De Spil), 447–453.

Gingerich, P., Raza, S., Arif, M., Anwar, M., and Zhou, X. (1994). New whale from the Eocene of Pakistan and the origin of cetacean swimming. *Nature* 368, 844–847. doi: 10.1038/368844a0

Greenwood, D. D. (1990). A cochlear frequency-position function for several species–29 years later. *J. Acoust. Soc. Am.* 87, 2592–2605. doi: 10.1121/1.399052

Heffner, R. S., and Heffner, H. E. (1992). "Evolution of sound localization in mammals," in *The Evolutionary Biology of Hearing*, eds D. B. Webster, R. R. Fay, and A. N. Popper (New York, NY: Springer), 691–715. doi: 10.1007/978-1-4612-2784-7_43

Henson, O. W. Jr. (1965). The activity and function of the middle ear muscles in echolocating bats. *J. Physiol.* 180, 871–887. doi: 10.1113/jphysiol.1965.sp007737

Ingmanson, D. E., and Wallace, W. J. (1973). *Oceanology: An Introduction*. Belmont: Wadsworth Publishing Co., Inc.

Kandel, B. M., and Hullar, T. E. (2010). The relationship of head movements to semicircular canal size in cetaceans. *J. Exp. Biol.* 213(Pt. 7), 1175–1181. doi: 10.1242/jeb.040105

Kastelein, R. A., Bunskoek, P., Hagedoorn, M., Au, W. W. L., and de Haan, D. (2002). Audiogram of a harbor porpoise (*Phocoena phocoena*) measured with narrow-band frequency-modulated signals. *J. Acoust. Soc. Am.* 112, 334–344. doi: 10.1121/1.1480835

Kastelein, R. A., Helder-Hoek, L., Cornelisse, S., von Benda-Beckmann, A. M., Lam, F. A., De Jong, C. A. F., et al. (2020). Lack of reproducibility of temporary hearing threshold shifts in a harbor porpoise after exposure to repeated airgun sounds. *J. Acoust. Soc. Am.* 148, 556–565. doi: 10.1121/10.0001668

Ketten, D. R. (1992). "The marine mammal ear: Specializations for aquatic audition and echolocation," in *The Evolutionary Biology of Hearing*, eds D. Webster, R. Fay, and A. Popper (New York: Springer-Verlag), 717–754. doi: 10.1007/978-1-4612-2784-7_44

Ketten, D. R. (1994). Functional analyses of whale ears: adaptations for underwater hearing. *I.E.E.E Underwater Acoust.* 1, 264–270.

Ketten, D. R. (1997). Structure and function in whale ears. *Bioacoustics* 8, 103–136. doi: 10.1080/09524622.1997.9753356

Ketten, D. R. (2000). "Cetacean ears," in *Hearing by Whales and Dolphins*, eds W. W. L. Au, A. N. Popper, and R. R. Fay (Heidelberg: Springer), 43–108. doi: 10.1007/978-1-4612-1150-1_2

Ketten, D. R., and Mountain, D. C. (2011). *Final Report: Modeling Minke Whale Hearing, IOGP SML Joint Industry Programme*. London. 1–30. doi: 10.1002/9781118561546.ch1

Ketten, D. R., Simmons, J., Riquimaroux, H., Cramer, S., and Arruda, J. (2012). Critical cranial and cochlear structures in echolocators. *Proc. Inst. Acoust.* 34, 572–577.

Ketten, D. R., Skinner, M., Wang, G., Vannier, M., Gates, G. A., and Neely, J. G. (1998). In vivo measures of cochlear length and insertion depths of nucleus® cochlear implant electrode arrays. *Ann. Otol. Rhinol. Laryngol.* 107, 1–16.

Ketten, D. R., and Wartzok, D. (1990). "Three-dimensional reconstructions of the dolphin ear," in *Sensory Abilities of Cetaceans: Field and Laboratory Evidence.* Proceeding NATO ASI Series A Life Science, eds J. Thomas and R. Kastelein (New York, NY: Plenum Press), 196.

Kick, S. A., and Simmons, J. A. (1984). Automatic gain control in the bat's sonar receiver and the neuroethology of echolocation. *J. Neurosci.* 4, 2725–2737. doi: 10.1523/JNEUROSCI.04-11-02725.1984

Koopman, H. N., Budge, S. M., Ketten, D. R., and Iverson, S. J. (2006). The topographical distribution of lipids inside the mandibular fat bodies of odontocetes: remarkable complexity and consistency. *IEEE J. Ocean Engin.* 31, 95–106. doi: 10.1109/joe.2006.872205

Kössl, M., and Vater, M. (1995). "Cochlear structure and function in bats," in *Hearing by Bats*, eds R. R. Fay and A. N. Popper (New York, NY: Springer), 191–234. doi: 10.1007/978-1-4612-2556-0_5

Maison, S. F., and Liberman, M. C. (2000). Predicting vulnerability to acoustic injury with a noninvasive assay of olivocochlear reflex strength. *J. Neurosci.* 20, 4701–4707. doi: 10.1523/JNEUROSCI.20-12-04701.2000

Manoussaki, D., Chadwick, R. S., Ketten, D. R., Arruda, J., Dimitriadis, D., and O'Malley, J. T. (2008). The influence of cochlear shape on low-frequency hearing. *Proc. Natl. Acad. Sci. U.S.A.* 105, 6162–6166. doi: 10.1073/pnas.0710037105

Miller, B. S., Newburg, S. O., Zosuls, A. L., Mountain, D. C., and Ketten, D. R. (2006). "Biomechanics of dolphin hearing. A comparison of middle and inner

ear stiffness with other mammalian species," in *Auditory Mechanisms: Processes and Models*, ed. A. L. Nuttal (Singapore: World Scientific), 121–124.

Nachtigall, P. E., Supin, A. Y., Pacini, A. F., and Kastelein, R. A. (2018). Four odontocete species change hearing levels when warned of impending loud sound. *Integr. Zool.* 13, 2–20.

Nadol, J. B. Jr. (1988). Quantification of human spiral ganglion cells by serial section reconstruction and segmental density estimates. *Am. J. Otolaryngol.* 9, 47–51. doi: 10.1016/s0196-0709(88)80007-3

Norris, K. S. (1969). "The echolocation of marine mammals," in *The Biology of Marine Mammals*, ed. H. T. Andersen (London: Academic Press), 391–424.

Nummela, S. (1995). Scaling of the mammalian middle ear. *Hear. Res.* 85, 18–30. doi: 10.1016/0378-5955(95)00030-8

Oelschlager, H. A. (1986). Comparative morphology and evolution of the otic region in toothed whales. *Am J. Anat.* 177, 353–368. doi: 10.1002/aja.1001770306

Puria, S. (2020). Middle ear biomechanics: smooth sailing. *Acoust. Today* 16, 27–35. doi: 10.1121/AT.2020.16.3.27

Pye, A. (1966). The Megachiroptera and Vespertilionoidea of the Microchiroptera. *J. Morph.* 119, 101–120. doi: 10.1002/jmor.1051190202

Reidenberg, J. S., and Laitman, J. T. (2018). Anatomy of underwater sound production with a focus on ultrasonic vocalization in toothed whales including dolphins and porpoises. *Handbook Behav. Neurosci.* 25, 509–519. doi: 10.1016/b978-0-12-809600-0.00047-0

Reysenbach de Haan, F. W. (1956). Hearing in whales. *Acta Otolaryngol. Suppl.* 134, 1–114. doi: 10.1007/978-1-4612-1150-1_1

Rossing, T. D., and Fletcher, N. H. (2004). *Principles of Vibration and Sound*. New York: Springer. doi: 10.1007/978-1-4757-3822-3_13

Schuknecht, H. F. (1953). Technique for study of cochlear function and pathology in experimental animals. *Arch. Otolaryngol.* 58, 377–397. doi: 10.1001/archotol.1953.00710040399001

Schuknecht, H. F. (1993). *Pathology of the Ear*. Malvern, PA: Lea & Febiger, 7–21.

Siemers, B. M., and Schnitzler, H.-U. (2004). Echolocation signals reflect niche differentiation in five sympatric congeneric bat species. *Nature* 429, 657–661. doi: 10.1038/nature02547

Simmons, A. M., Ertman, A., Hom, K. N., and Simmons, J. A. (2018). Big brown bats (*Eptesicus fuscus*) successfully navigate through clutter after exposure to intense band-limited sound. *Sci. Rep.* 8:13555. doi: 10.1038/s41598-018-31872-x (2018)

Simmons, A. M., Hom, K. N., and Simmons, J. A. (2017). Big brown bats (*Eptesicus fuscus*) maintain hearing sensitivity after exposure to intense band-limited noise. *J. Acoust. Soc. Am.* 141, 1481–1489. doi: 10.1121/1.4976820

Simmons, A. M., Hom, K. N., Warnecke, M., and Simmons, J. A. (2016). Broadband noise exposure does not affect hearing sensitivity in big brown bats (*Eptesicus fuscus*). *J. Exp. Biol.* 219, 1031–1040. doi: 10.1242/jeb.135319

Simmons, J. A. (2017). Theories about target ranging in bat sonar. *Acoust. Today* 13, 43–51.

Simmons, J. A., Ferragamo, M., Moss, C. F., Stevenson, S. B., and Altes, R. A. (1990). Discrimination of jittered sonar echoes by the echolocating bat. *Eptesicus fuscus*: the shape of target images in echolocation. *J. Comp. Physiol. A.* 167, 589–616.

Slabbekoorn, H. (2004). Habitat-dependent ambient noise: consistent spectral profiles in two African forest types. *J. Acoust. Soc. Am.* 116, 3727–3733. doi: 10.1121/1.1811121

Southall, B., Finneran, J., Reichmuth, C., Nachtigall, P., Ketten, D., Bowles, A., et al. (2019). Marine mammal noise exposure criteria: auditory weighting functions and TTS/PTS onset. *Aquat. Mamm.* 45, 125–232. doi: 10.1578/AM.45.2.2019.125

Spoor, F., Bajpai, S., Hussain, S. T., Kumar, K., and Thewissen, J. G. (2002). Vestibular evidence for the evolution of aquatic behaviour in early cetaceans. *Nature* 417, 163–166. doi: 10.1038/417163a

Suga, N., and Jen, P. H.-S. (1975). Peripheral control of acoustic signals in the auditory system of echolocating bats. *J. Exp. Biol.* 62, 277–311. doi: 10.1242/jeb.62.2.277

Surlykke, A., and Moss, C. F. (2000). Echolocation behavior of big brown bats, *Eptesicus fuscus*, in the field and the laboratory. *J. Acoust. Soc. Am.* 108, 2419–2429. doi: 10.1121/1.1315295

Tubelli, A., and Ketten, D. (2019). The role of material properties in cetacean hearing models: knowns and unknowns. *Aquat. Mamm.* 45, 717–732. doi: 10.1578/AM.45.6.2019.717

Tubelli, A., Zosuls, A., Ketten, D., Yamato, M., and Mountain, D. (2012). A prediction of the minke whale (*Balaenoptera acutorostrata*) middle-ear transfer function. *J. Acoust. Soc. Am.* 132, 3263–3272. doi: 10.1121/1.4756950

Tyack, P. L., Johnson, M., Aguilar Soto, N., Sturlese, A., and Madsen, P. T. (2006). Extreme diving of beaked whales. *J. Exp. Biol.* 209, 4238–4253. doi: 10.1242/jeb.02505

Urick, R. J. (1983). *Principles of Underwater Sound*. New York, NY: McGraw-Hill.

Vater, M. (2004). "Cochlear anatomy related to bat echolocation," in *Echolocation in Bats and Dolphins*, eds J. A. Thomas, C. F. Moss, and M. Vater (Chicago, IL: University of Chicago Press), 99–103.

Veselka, N., McErlain, D., Holdsworth, D., Eger, J. L., Chhem, R. K., Mason, M. J., et al. (2010). A bony connection signals laryngeal echolocation in bats. *Nature* 463, 939–942. doi: 10.1038/nature08737

von Békésy, G. (1960). *Experiments in Hearing*. New York, NY: McGraw–Hill.

von Uexküll, J. (1957). "A stroll through the worlds of animals and men: a picture book of invisible worlds," in *Instinctive Behavior: The Development of a Modern Concept, Edited and Translated*, ed. C. H. Schiller (New York, NY: International Universities Press), 5–80.

Wartzok, D., and Ketten, D. R. (1999). "Marine mammal sensory systems," in *Biology of Marine Mammals*, eds J. Reynolds and S. Rommel (Washington DC: Smithsonian Institution Press), 117–175.

Wenz, G. M. (1962). Acoustic ambient noise in the ocean: spectra and sources. *J. Acoust. Soc. Am.* 34, 1936–1956. doi: 10.1121/1.1909155

West, C. D. (1985). The relationship of the spiral turns of the cochlea and the length of the basilar membrane to the range of audible frequencies in ground dwelling mammals. *J. Acoust. Soc. Am.* 77, 1091–1101. doi: 10.1121/1.392227

Wever, E. G., McCormick, J., Palin, J., and Ridgway, S. (1972). Cochlear structure in the dolphin, *Lagenorhynchus obliguidens*. *Proc. Nat. Acad. Sci. U.S.A.* 69, 657–661. doi: 10.1073/pnas.69.3.657

Wever, E. G., McCormick, J. G., Palin, J., and Ridgway, S. (1971a). The cochlea of the dolphin, *Tursiops truncatus*: Hair cells and ganglion cells. *Proc. Nat. Acad. Sci. U.S.A.* 68, 2908–2912. doi: 10.1073/pnas.68.12.2908

Wever, E. G., McCormick, J. G., Palin, J., and Ridgway, S. (1971b). The cochlea of the dolphin, *Tursiops truncatus*: The basilar membrane. *Proc. Nat. Acad. Sci. U.S.A.* 68, 2708–2711. doi: 10.1073/pnas.68.11.2708

Yamato, M., Ketten, D. R., Arruda, J., Cramer, S., and Moore, K. (2012). The auditory anatomy of the minke whale (*Balaenoptera acutorostrata*): a potential fatty sound reception pathway in a baleen whale. *Anat. Rec.* 295, 991–998. doi: 10.1002/ar.22459

**Conflict of Interest:** The reviewer AP declared an editorial collaboration with one of the authors, DK, to the handling editor.

The remaining authors declare that the research was conducted in the absence of any commercial or financial relationships that could be construed as a potential conflict of interest.

**Publisher's Note:** All claims expressed in this article are solely those of the authors and do not necessarily represent those of their affiliated organizations, or those of the publisher, the editors and the reviewers. Any product that may be evaluated in this article, or claim that may be made by its manufacturer, is not guaranteed or endorsed by the publisher.